

CHARACTERIZATION AND ORIGIN OF 1:1 PHYLLOSILICATES WITHIN PELOIDS OF THE RECENT, HOLOCENE AND MIOCENE DEPOSITS OF THE CONGO BASIN

A. WIEWIÓRA,¹ B. LACKA,¹ P. Giresse²

¹ Institute of Geological Sciences, Polish Academy of Sciences, al. Zwirki i Wigury 93, 02-089 Warszawa, Poland

² Laboratoire de Sédimentologie et Géochimie Marines, Université de Perpignan, 52, Avenue de Villeneuve, 66860 Perpignan, France

Abstract—The grey-green peloids from the Miocene period to Recent fine-grained deposits on the continental shelf close to Congo-Zaire River mouth were studied by X-ray transmission diffractometry (XRD), SEM and by EDAX. The peloids have multiphase heterogenous mineral composition. Their most important constituents are detrital minerals like kaolinite, quartz, goethite, 7 Å phases with $d(001) \approx 7.3$ Å, and in more matured grains—nontronite. The $d(060)$ values were used to estimate the general composition of phyllosilicate phases to compare with the composition determined by EDAX. It has been found that $d(060)$ equal to 1.504 Å is common for Fe³⁺-bearing kaolinite, which is quite abundant for the Recent peloids. The $d(060)$ equal to 1.535 Å and 1.55 Å is characteristic for the di-trioctahedral and trioctahedral 1:1 phases, which are abundant within the more evolved Miocene peloids. Nontronite is characterized by $d(060)$ equal to 1.524 Å within concordance with its highly ferrous composition, and partly by its potassic interlayer. It shows cabbage-like nanostructures proving neoformational origin of this mineral in the marine environment.

It has been shown that areas of the low sedimentation rate within the Congo Basin were favorable for the mineral changes and neoformation. For the Holocene vertical profile, we observed levels of slower sedimentation rates. The evolution is expressed by the disappearance of kaolinite at the expense of other 7 Å phases and nontronite. Although more advanced stages of maturation of the studied phases were observed in older peloids (10⁴ to 10⁷ y), one cannot detect a linear relationship of these processes with burial.

Key Words—1:1 phyllosilicate, Chemical composition, Nontronite, Peloids, X-ray diffraction.

INTRODUCTION

Recent coastal sediments from the intertropical continental margin contained mineralized fecal pellets with various compositions. The most likely environment for their origin is shallow marine, near a river mouth, which could have supplied the organic matter and the necessary Fe. Such an occurrence is of special interest for the many investigators of sedimentary ironstones as mineralized fecal pellets may represent initial stages of the formation of Fe-containing phyllosilicates.

On the Congolese shelf, the bottom waters from 40 m to 10 m display consistent temperatures of approximately 17 °C. Contrary to the generalization that the deposits, where the 7 Å phase in green grains appears to form, are composed of porous sediments having a particle size >500 μm (Odin and Sen Gupta 1988), the green grains on the African Atlantic margin consist primarily of fecal pellets, or infillings or coatings of porous bioclastic debris. For both cases, these grains are closely related to muddy sediment, favorable for mud-eaters. Some associations with coarse deposits are related to reworking processes because of the higher energy of shallow-water movement, and the 18,000 BP low-stand green sands of the Congolese outer shelf are one of the major examples of such a process.

While neoformation of the ferruginous smectites, glauconite precursors in fecal peloids within the marine sediments of the intertropical continental margins has been documented (Giresse et al. 1987, 1988, 1992), the crystal chemistry and origin of 7 Å phases remains obscure. The precise definition of these phases meets several difficulties: 1) mineral and chemical heterogeneity related to particle sizes and density of peloids (Giresse et al. 1987, 1988); 2) heterogeneity of the associated phases within different phyllosilicates, such as neoformed smectite, inherited detrital kaolinite, micas and chlorite, and also the possible alteration product of 1:1 mineral phases (Odin 1988), goethite and amorphous iron hydroxides, a problematic intermediate smectite-swelling chlorite and low temperature pyrophyllite-like minerals (Odin 1988); 3) poor crystallinity of most phases, generally metastable within the deposition environment; and 4) geographic, depositional environment and age variation reflected within various interactions between heritage, diagenetic neoformation and transformation.

The 7 Å phases, which are difficult to classify, are also reported within the sediment cement (Parron 1989). However, the phases do not necessarily reflect the composition of peloids. The mentioned difficulties for precisely defining 7 Å phases within peloids of verdine facies (Odin 1985) has resulted in a number

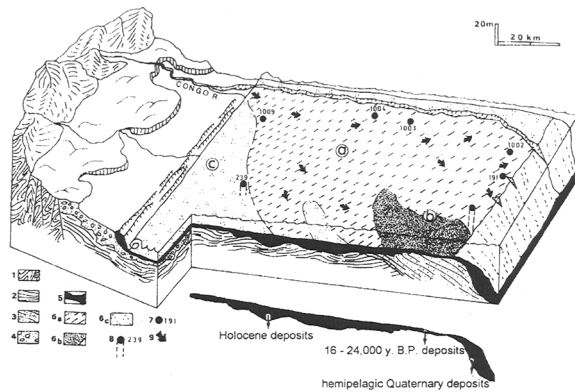


Figure 1. Location and geological setting of study area. Key: 1 = Precambrian basement; 2 = Ceno-Mesozoic; 3 = Miocene; 4 = Plio-Pleistocene; 5 = Holocene; 6 = areas of Recent superficial sediments: a = kaolinite transformation, b = glauconitization, c = sandy silt sedimentation; 7 = Location of samples from superficial deposits; 8 = location of drillings; 9 = transport directions. On the cross-section: The Holocene deposits contain 3 to 15 weight % of green grains (prevailing 1:1 minerals), 16-24000 y.B.P. deposits include 50 to 80 weight % of green grains (prevailing 2:1 minerals) and hemipelagic Quaternary deposits from the slope show only a few weight per cent of grains (reworked green grains from the outer shelf and *in situ* grey grains).

of names, such as 7 Å phyllite and verdine from Odin (1985), odinite from Bailey (1988), berthierine silicious from Parron (1989) and berthierine (Brindley 1982). In addition, Giresse et al. (1988) suggested other 7 Å phases. Therefore, further detailed studies of the 7 Å phases are desirable. This work will define the crystal-chemistry of the 7 Å di- and tri-octahedral phases and of the co-existing smectites found in peloids from the Congo continental margin sediments (Miocene to Recent).

MATERIALS AND METHODS

All of the samples, from the Miocene to Recent were collected from the continental shelf near the mouth of the Congo-Zaire River (Figure 1). The superficial bottom sediments were collected within the growing distance from the shore (numbers 1009, 1004, 1003, 1002 and 191) at a depth of 12 m, 45 m, 116 m, 120 m and 126 m (the 191 sample was previously studied by Giresse et al. 1988). The samples contain grey-green peloids, occasionally with a glossy surface, but usually with an earthy look, ovoid and mainly 100 to 200 µm in diameter. The Holocene samples (239) come from a 500 cm long core, taken from a depth of -30 m. They represent a series: -420 to 430 cm, -330 to 340 cm, -230 to 240 cm, -20 to 30 cm. The peloids are also grey-green, rarely dark green, and are associated with pseudo-oids of goethite. The Miocene samples come from the petroleum drilling from depth of -185 m, -220 m, -370 m, -520 m. The peloids are ovoid, but their pigmentation is more diverse:

grey-green, dark grey-green, rarely green-black. Giresse et al. (1992) gave a detailed description.

Peloids were isolated using a paramagnetic separator and then divided into lighter <1.53 g/cm³ and heavier >1.53 g/cm³ fractions, by means of density separation. The mineralogical composition of the peloid populations was studied by XRD, using 2 distinctly different techniques: 1) collective mini-samples of approximately 30 mg in weight, composed of several grains paramagnetically and/or density separated or hand picked, were analyzed. Co-Kα₁ radiation and a computerized data collection system with a DRX program from Vila et al. (1988) were used. To determine the b unit cell parameter of the 7 Å phases the decomposition of *d*(060) was performed; 2) the position sensitive detector (made by Inel, France), enabled X-ray analysis of the individual grains. This analysis supplemented the results obtained for powdered specimens composed of several grains from a given population. An ultrasonic bath cleaned the mud from fissures of the grains chosen for analysis. Diffractograms were recorded using Co-Kα₁ radiation, 0.5 × 0.5 slit of analysis and a collection time of 20 h. Samples were continuously rotated during analysis. The Diffractinel software V. 03/93 (Inel instrumentation électronique, France) was used to process the data.

The chemical composition of the individual phases was obtained by point analysis from the central part of flaky aggregates of 2 to 5 µm in diameter. Selected grains were hand crushed, put onto specimen holders and carbon coated. The other preparation techniques, such as polishing could not be used, since very fine and soft aggregates smear easily, thus making the distinction of minerals impossible. Analyses were performed using a 1 µm diameter beam and energy dispersive X-ray micro-analysis system (Link Analytical AN 10000/85S) combined with JSM 840A scanning electron microscope. The resolution of the Si(Li) detector was 143 eV at Mn-Kα. Beam energy was 15 keV. The standard correction program was used to convert the microprobe data to composition. For some cases, a special version of the quantitative computer program was employed. It was based on the apparent calculated concentration, taking into account the peak to background ratios rather than peak areas.

MINERAL COMPOSITION DERIVED FROM MULTI-GRAIN SAMPLES

Recent Superficial Sediments

Mineral composition of the peloids varies significantly with depth and distance from the shore. For the grains located farthest from the shore, for example within sample 1002 (Figure 1), kaolinite prevails over goethite (Figure 2a). With decreasing distance from the shore, such as samples 1004 and 1009 (Figure 1), the content of goethite clearly increases (Figure 2b and

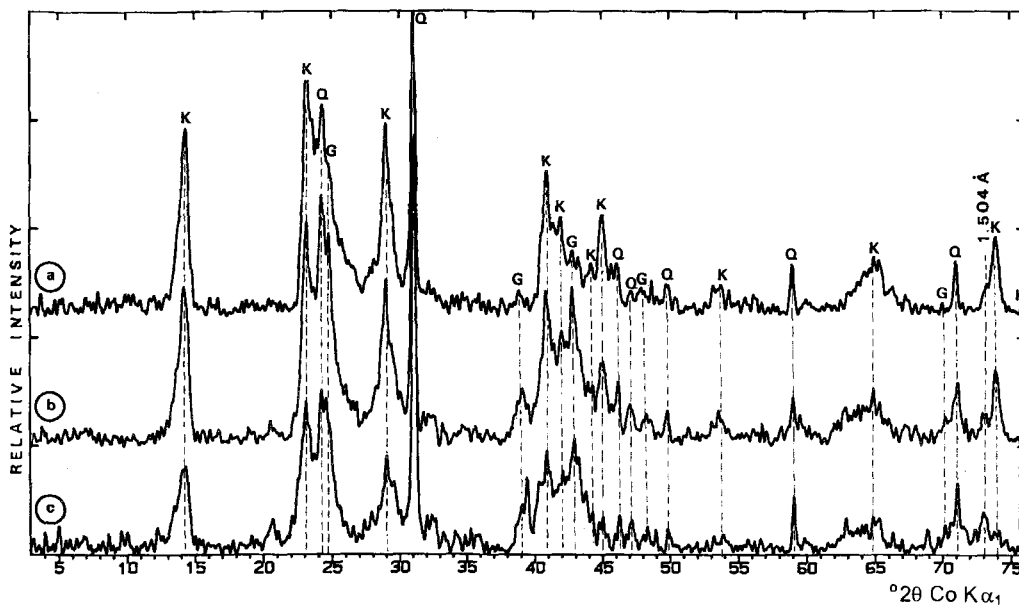


Figure 2. XRD patterns (background subtracted) of non-oriented aggregates of peloids from Recent superficial sediments. Samples: a = 1002, b = 1004, c = 1009. Key: K = kaolinite, Q = quartz, G = goethite, 1.504 Å = $d(060)$ of Fe-kaolinite.

2c) and kaolinite decreases. The disappearance of kaolinite $d(060)$ reflections for Figures 2a, 2b and 2c is accompanied by appearance of the other $d(060)$ reflection characterized by $d = 1.504$ Å.

The absence of $d(001)$ mica (illite) reflection and of $d(060)$ reflection of kaolinite and the presence of the important 7 Å peak permits us to suggest the occurrence of the dioctahedral 7 Å phase other than kaolinite (Figure 2b and 2c). The reasonable explanation for the appearance of this phase in the goethite samples is the transformation of highly particulated kaolinite fractions into Fe-bearing kaolinite.

X-ray patterns of several populations of grains (grey green, dark green) studied from sample 191, which was located close to the area of the glauconite formation, proved reflections ≈ 1.53 Å and ≈ 1.55 Å, thus indicating trioctahedral phases in addition to the dioctahedral kaolinite and Fe-bearing kaolinite. These reflections are displayed in the proximity of the 1.54 Å quartz reflection. Phases represented by these reflections will be studied in the quartz and goethite-free grains from Miocene deposits. For sample 191, we observed the occurrence of smectite (Figure 3), which is missing within peloids from the other locations. Unit cell parameter b equal to 9.14 Å, recalculated from $d(060) = 1.524$ Å, indicates a nontronitic character of smectite. Upon heating to 300 °C, the $d(001)$ spacing of the mineral collapses, but when exposed to air, it showed partial progressive re-expansion. This indicates non-homogenic distribution of cations and charges within and between the layers. Observation of the effect of collapse and re-expansion is impaired by the fact that the $d(001)$ intensity is relatively low in por-

tion to (02, 11) band intensity. Sometimes only hk bands are recorded (Brindley 1980), which is a common characteristic of many nontronites.

Holocene Sediments From Core 239, (−30 m)

Mineral composition of the grey-green peloids in the 4 studied horizons (Figure 4) is similar to that of samples 191 from the Recent superficial sediments. For all of the 4 samples studied, the major minerals are smectite, 7 Å phases, quartz and goethite. The X-ray characteristics of the 7 Å phases is different from that of kaolinite. The 7 Å peak is smaller and broader than the 7 Å peak of kaolinite observed for Recent peloids. In the $d(060)$ region, the 1.488 Å peak of kaolinite is almost completely absent, but another peak appeared that shifted toward smaller angles. As in Recent sediments, they are overlapped and masked by the 1.541 Å peak of quartz.

From the relative intensity of basal reflections of the smectite and of the 7 Å phases, the evolution of grains is expressed by the upward increment of the smectite content and a decreased kaolinite content on behalf of the 7 Å Fe-bearing phase.

Miocene Sediments

From the X-ray study, it appears that nontronite is the major constituent of the light <1.53 g/cm³ fractions while 7 Å phases, especially kaolinite, are more important within heavier fractions. Non phyllosilicate minerals, like goethite and quartz are less important (Figure 5). For the $d(060)$ range, diffractograms envisaged a distinct heterogeneity of mineral composition (Figure 6). However, within the multi-grain sam-

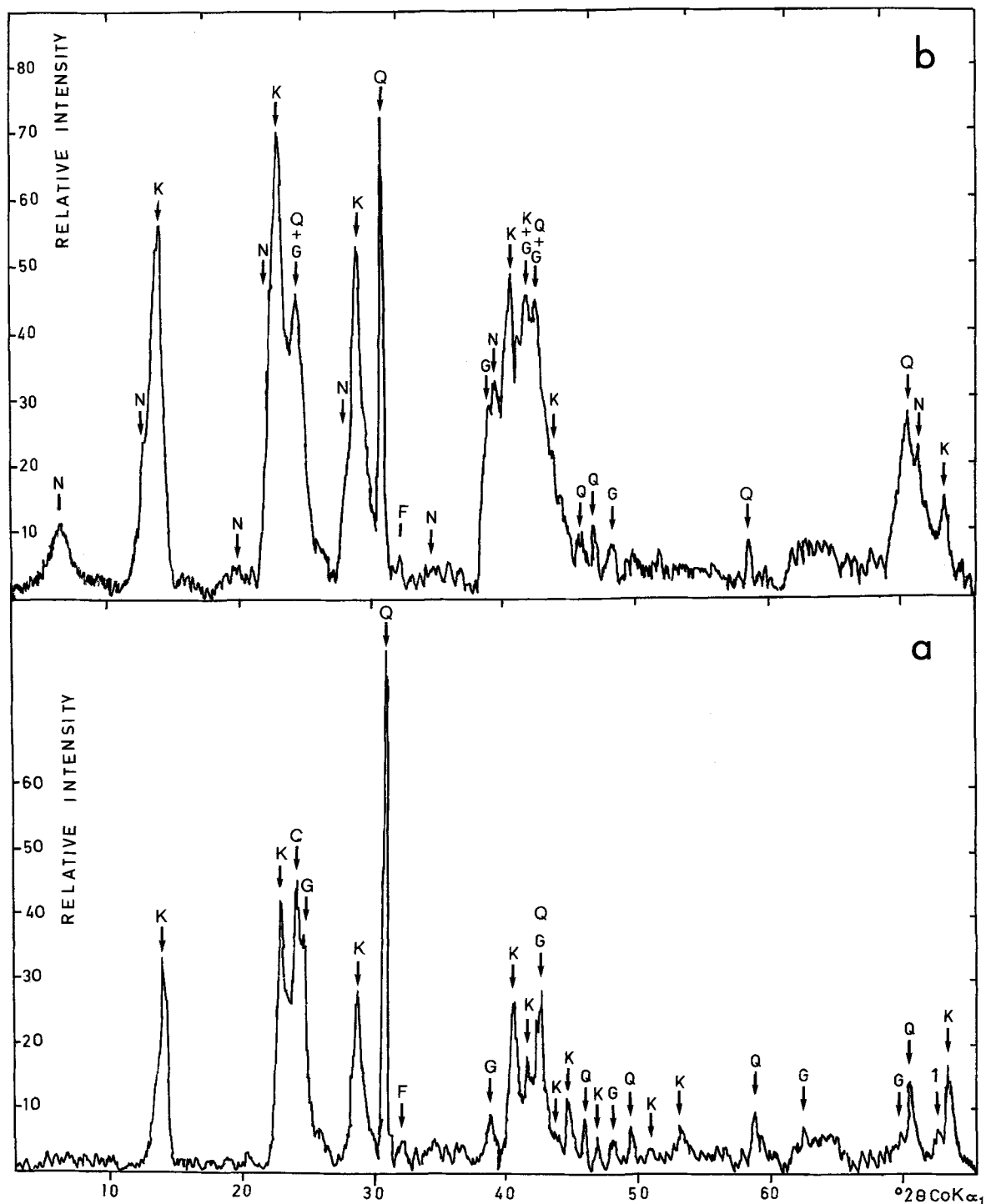


Figure 3. XRD patterns (background subtracted) of non-oriented aggregates of peloids from Recent superficial sediments. Comparison of: a = nontronite-free sample 1004; b = nontronite containing sample 191. Key: K = kaolinite; Q = quartz; N = nontronite; G = goethite; and F = feldspar; 1.504 Å = $d(060)$ of Fe-bearing kaolinite.

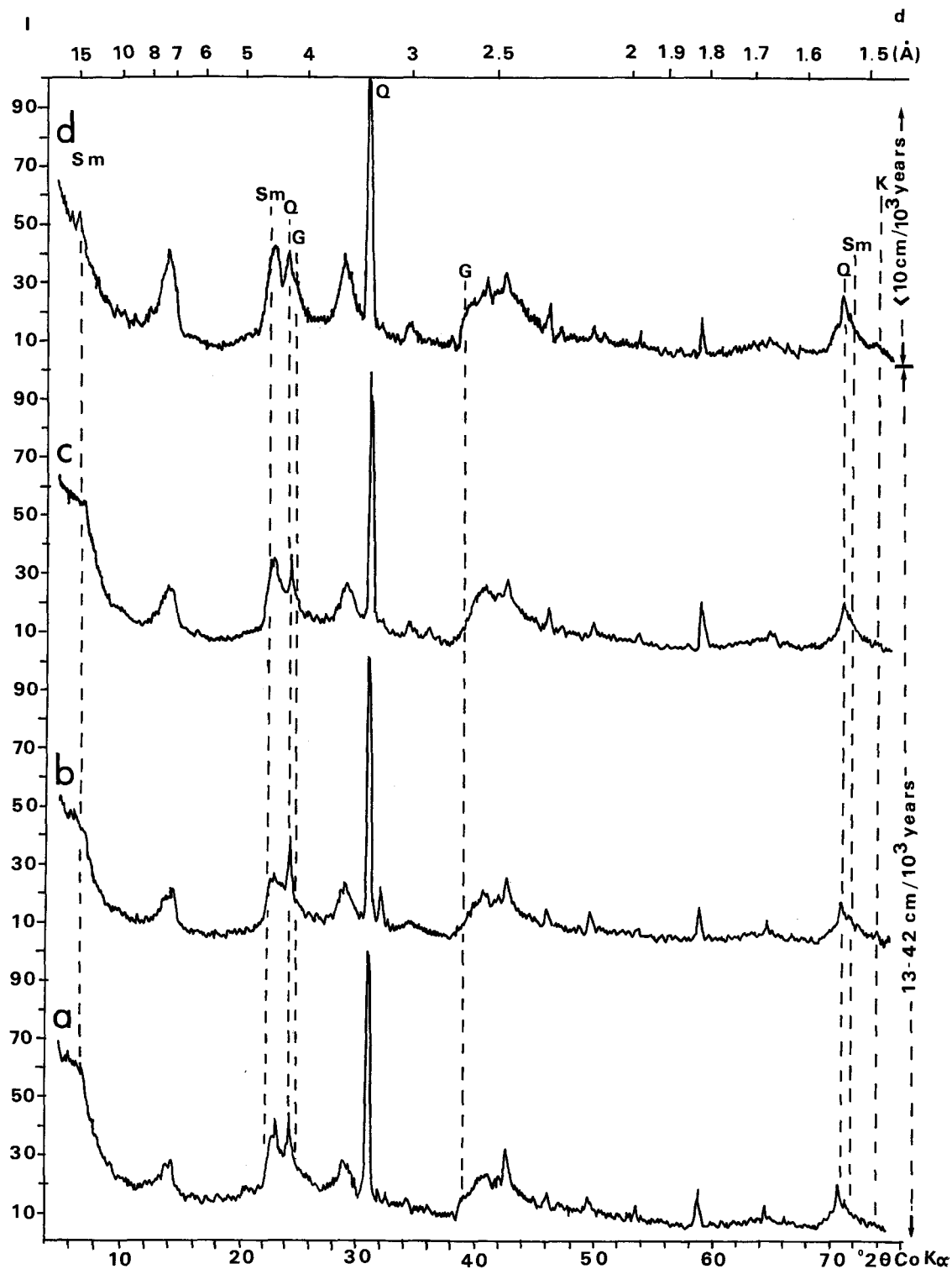


Figure 4. XRD patterns of non-oriented aggregates of Holocene grains (core 239 at -30 m): a = (-530 -540 cm); b = (-230 -240 cm); c = (-110 -140 cm); d = (-20 -30 cm). Key: N = nontronite; K = $d(060)$ of kaolinite; Q = quartz; G = goethite; and non marked peaks = 7 Å phases.

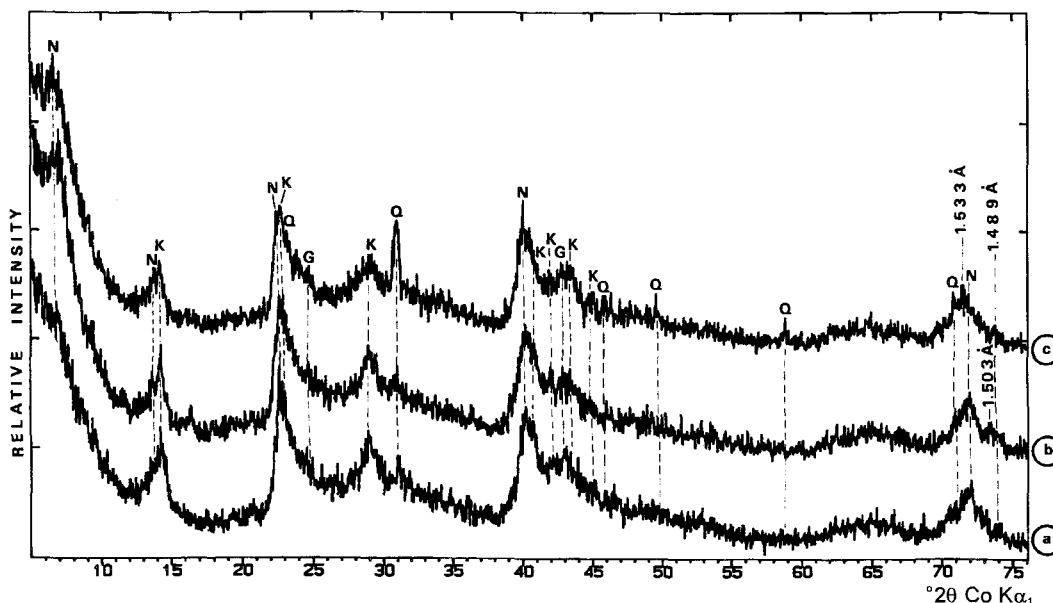


Figure 5. XRD patterns of non-oriented aggregates of the Miocene peloids: a = collective sample; b = grey-green grains from density separated sample 185; c = grey-green grains from density separated sample 220. Key: N = nontronite; Q = quartz; and non labeled peaks = 7 Å phases.

ple, nontronite prevails over 7 Å phases (Figure 6, curve 1). The -185 m sample (Figure 6, curve 2) appeared good for precise measurements of $d(060)$ spacing of various 1:1 phases. Other than kaolinite peak

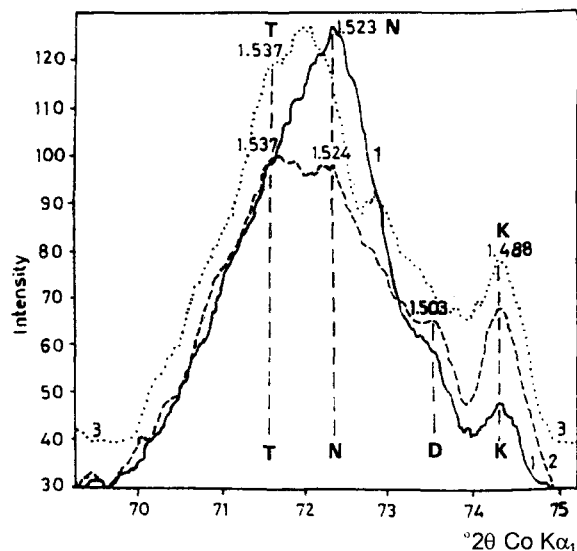


Figure 6. XRD patterns for the $d(060)$ region for non-oriented aggregates of Miocene grains: 1 = collective Miocene grey green grains; 2 = grey-green grains from sample -185 m; 3 = grey green grains from sample -370 m. Goniometer speed $10^\circ/\theta$, Co-K α_1 radiation and pattern smoothing were applied. $d(060)$ values indicate: K = kaolinite; T = 7 Å phase; N = nontronite. D = 7 Å phases relatively close to kaolinite; and G = goethite.

(1.488 Å), there are relatively distinct peaks, at 1.537 Å and 1.503 Å. The spectrum was deconvoluted to better show the individual peaks, using Pearson interactive approximation (Figure 7). The broadest peak is that of nontronite, the narrowest is of detrital kaolinite, and the intermediate peaks are the other 7 Å phases.

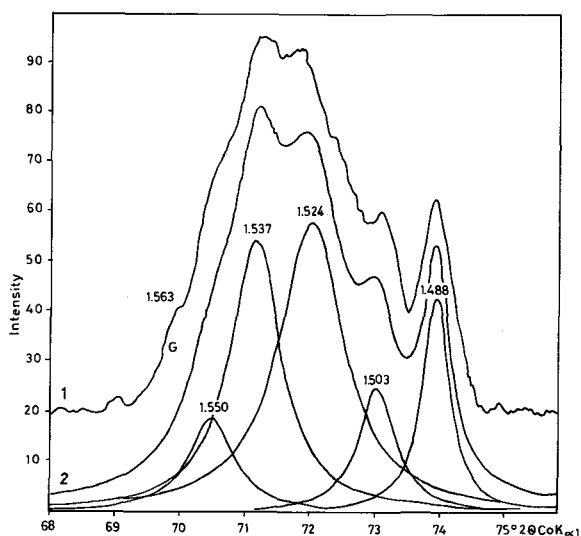


Figure 7. Deconvolution of the $d(060)$ region of the diffraction pattern of -185 m sample, recorded with Co-K α_1 radiation and goniometer speed $10^\circ/\theta$: 1 = curve 2 from Figure 6; 2 = cumulative curve from individual peaks obtained by deconvolution of the curve 1. Values of interlayer spacings obtained by spectrum deconvolution are given over the individual peaks; and G = goethite.

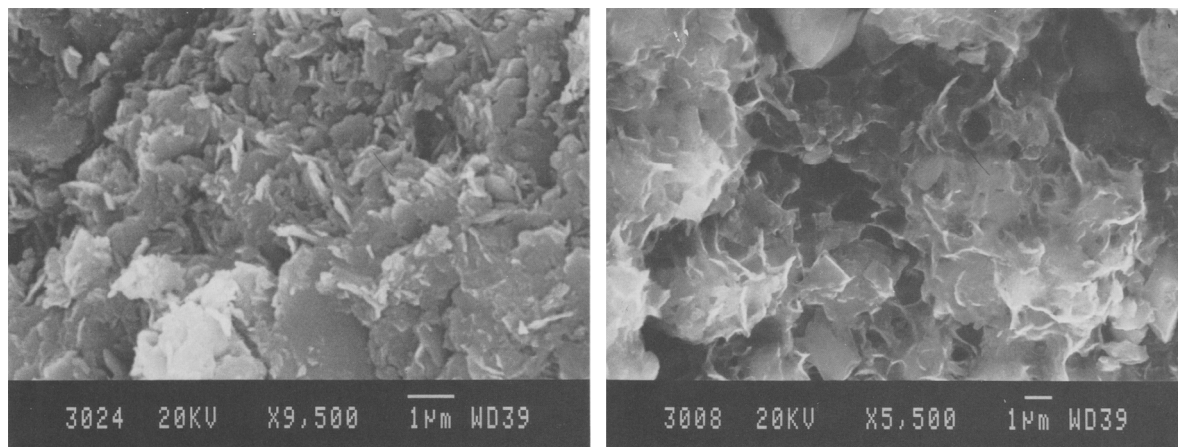


Figure 8. Cabbage-like structure of neoformed nontronite coated by irregular and larger flakes on the same mineral sample. Magnification is on the photos a and b.

The full width at half maximum (FWHM) of the peaks agree with particle size observations under scanning microscope. Fine particles with a relatively high content of Fe and Mg within the structure may be attributed to 7 Å trioctahedral phases. The very coarse particles are characterized by a highly aluminous composition and belong to kaolinite. The finest particles, with a very limited number of structural layers, are those forming cabbage-like neoformed assemblages of nontronite (Figure 8).

Summary of Multi-Grain Samples Analysis

From X-ray study of average, multi-grain samples, it appears that Recent green grains show an abundance of detrital minerals, such as kaolinite, quartz and goethite (Figure 2). Goethite can also be formed later as a marine oxidation product.

Changes within the spatial distribution of mineral grains for sediments with increasing distance from the shore and river mouth were demonstrated. The mineral distribution vary in a progressive manner depending upon transportation processes from the Congo-Zaire River mouth. The studied deposits, location 1009 at -45 m (Figure 2) with high kaolinite content, represent the highest sedimentation rate. The peloids are less evolved and differentiated than those from the area of lower sedimentation rate, closer to the glauconite formation area. The abundance of goethite in nearshore sediments indicates oxidizing conditions.

For the Holocene deposit, a negative correlation between the burial depth and the appearance of smectites was observed. Its appearance and the disappearance of kaolinite suggest that these processes are related to the sedimentation rate. Mineralogical transformation can be affected by the cationic exchange at sea-water sediment interface during a period of slow sedimentation (<10 cm/10³ years). Quartz and goethite persist and

are present in all samples studied (Figure 4). However, within the Miocene green grains, the quartz mostly disappeared (Figure 5).

For the average composition of the Miocene grains, nontronite prevails or is equal in content to 7 Å phases. Miocene grains compared to Recent and Holocene epochs evidenced the burial-induced process, but there is no strong positive correlation between their evolution and depth.

STUDIES ON INDIVIDUAL GRAINS FROM MIOCENE DEPOSITS

Mineralogy

The grains from Miocene sediments have been analyzed with 14 from the light grey-green population of grains and 9 dark green to black ones. Within each population multiphase grains composed of 7 Å trioctahedral, 7 Å dioctahedral phases and nontronite with a minor admixture of quartz prevail (Figure 9a and 9b). However, there are a few grains containing almost totally nontronite (Figure 9c). Mineral composition differentiation between individual grains constitutes a significant advancement for the study of the green grains. The diffraction patterns confirmed the mineral composition determined for multi-grain samples. Also, we were able to present a better diffraction pattern of nontronite (Figure 9c). The value 1.524 Å indicates a high Fe content within its structure (Figure 10). This high Fe content has been confirmed by EDAX determination. EDAX analysis also shows a considerable content of K. However, diffraction patterns showed a rather broad *d*(001) reflection for nontronite (Figure 9c). This broadening of the *d*(001) reflection might have previously been incorrectly ascribed to the interstratified illite/smectite phase. But presently, it is due to the mixed cations within the interlayer space (Table

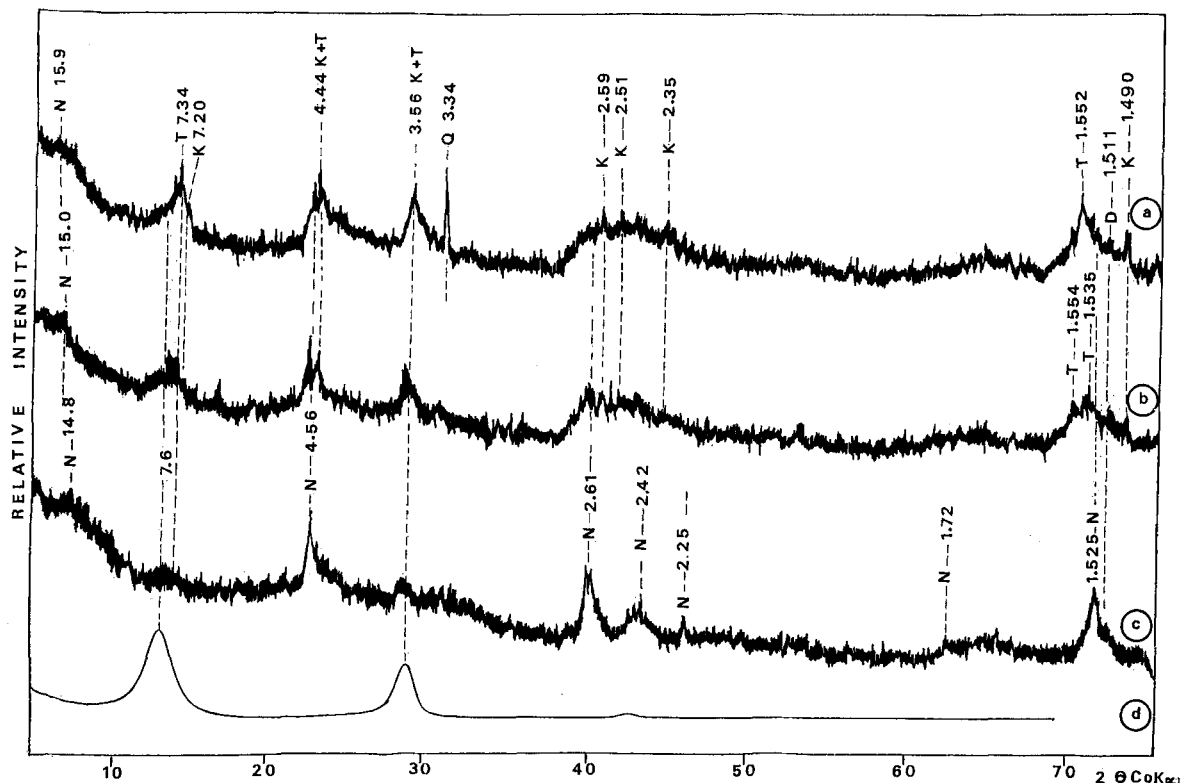


Figure 9. XRD patterns of three (a, b, c) single Miocene grains recorded with the use of PSD - 120, Co-K α_1 radiation, and d = simulated pattern of 85/15 Fe-bearing serpentine/glaucinite interstratification. Key: N = nontronite, T = 7 Å dioctahedral close to trioctahedral and trioctahedral 1:1 phases; Q = quartz; D = dioctahedral 7 Å phases close to kaolinite, d spacings in Å are given.

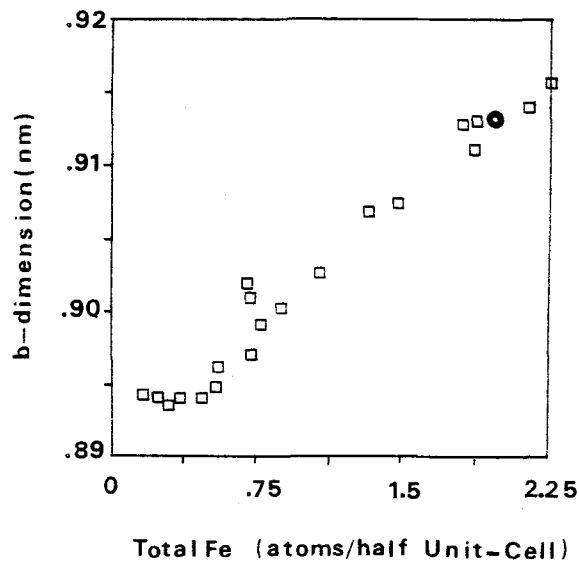


Figure 10. Relationship between b dimension and total octahedral Fe in smectites (Brigatti 1985; Stucki 1988, p 652). Key: squares = original projections of Brigatti; and circle = projection from this work.

1), rather than illite/smectite interstratification. To clarify this situation, we selected a grain displaying a relatively narrow $d(001)$ peak at 12.6 Å and a series of strong reflections with spacings identical to those in Figure 9c. Subsequently, we replaced K with Ca. The Ca-saturated sample was subjected to chemical analyses using EDAX (Table 1, column 2). However, only some of the K was replaced by Ca and only part of the structure expanded to ≈ 15 Å. Such limited exchange of Ca for K indicates that K is fixed strongly within the nontronite structure. The fixation of K is the first important sign of initialization of the glauconitization process of highly ferruginous nontronite.

The separation of the 7 Å phases is more complicated. The XRD data indicate 2 distinct phases, namely that having $d(060) = 1.535$ Å and the other, with $d(060) = 1.55$ Å, which are from the 7 Å dioctahedral phase. These 2 different 7 Å phases may represent various stages of ferruginous 1:1 minerals formation. Observations of $d(001)$ reflections showed the broadening of these reflections with changing composition. At times, the reflection was split into two maxima: 1) approximately 7.3 Å; and 2) approximately 7.6 to 7.9 Å. It is possible that the broadening of the $d(001)$ re-

Table 1. Average chemical composition and structural formulae of smectites in 3 Miocene grains. Each analysis represents the average value from 8 or more points.

Element	-185 m		-220 m
	1	2	3
Na	0.15	0.30	0.44
Mg	2.14	2.06	2.58
Al	4.17	5.10	5.65
Si	18.23	17.40	17.44
K	3.50	2.71	1.87
Ca	0.32	0.55	0.80
Ti	0.10	0.06	0.18
Fe	21.66	23.20	23.40
Si	3.16	2.98	2.91
Al(IV)	0.75	0.91	0.98
Fe ³⁺ (IV)	0.09	0.11	0.11
Fe ³⁺ (VI)	1.79	1.89	1.85
Mg	0.43	0.41	0.50
Ti	0.01	0.01	0.02
Na	0.03	0.06	0.09
K	0.44	0.33	0.22
Ca	0.04	0.07	0.09

flexion is due to particle size, which is finer for the trioctahedral than for the dioctahedral phases. Another possible explanation is that this peak is due to the random interstratification of 7 Å and 10 Å layers.

Such interstratification was observed in the Recent grains, namely in the sample 191, by HRTEM (Amouric et al. 1995). These authors proved formation of the 10 Å layers with glauconite type composition directly from the 7 Å trioctahedral layers. The latter were observed as formed from the Fe-containing 7 Å dioctahedral layers evidently via dissolution (Amouric et al. 1995). Diffractogram for 7 Å/10 Å interstratification with concentration probability coefficients $p_7 \text{ Å} = 0.85$, $p_{10 \text{ Å}} = 0.15$, Reichweite 0.5, in part ferruginous composition (one octahedral position occupied by Fe, two by Mg) and 0.8 K in the interlayer of glauconite 10 Å layers, calculated using Newmond 2 (v.2.0: 1985) from Reynolds, demonstrated strong reflections at 7.6 Å and 3.75 Å observed with in the experimental pattern in Figure 9. Thus, it is possible that both phenomena, the fine particle size and mixed-layering, are responsible for the very large and partly diffused $d(001)$ reflection in the region between 7.15 Å, which is typical for kaolinite, and 7.6 to 7.9 Å for glauconite. This was for glauconite, which was observed simultaneously with the appearance of $d(060) = 1.511 \text{ Å}$ (Figure 9). It may be argued that the bimodal intensity distribution of the $d(001)$ reflection may indicate transformation via local dissolution and crystallization, which should produce new phase fine particles within the host body, the kaolinite flakes.

The presence of 7 Å trioctahedral varieties indicates the possibility of the berthierization process, but this process could not have been completed for the sediments as formation of true berthierine seems possible

only under conditions of high pressure and temperature, characteristic for deep burial (Bhattacharyya 1983; Cotter 1992; Ijima and Matsumoto 1982; Velde 1989). Contrary to berthierization of 7 Å phases, glauconite formation is in progress, as shown by increasing growth of this mineral inside grains (Giresse et al. 1988; Amouric et al. 1995).

Chemical Composition of Individual Phyllosilicate Phases

The 7 Å PHASES. We have chosen 8 analyses of the most typical flakes in Recent and Miocene grains: 1) two size gradation of flakes (15 µm and 0.5 µm) from Recent superficial sediments (sample 191) (Table 2, columns 1 and 2) and four in the Miocene grains from different depths: -370 m, -520 m and -185 m and one from multi-grain sample (Table 2, columns 3, 4, 5 and 6). Each analysis represents average values from 8 or more points. All analyses show the presence of major elements for 1:1 minerals (Fe, Mg, Al and Si) but also have a minor content of K (1.1 to 0.5%), Na (0.3 to 0.15%) and Ca (0.5 to 0.3%), which are not common for them. Such elements may be attributed to a small admixture of nontronite, most frequently present within the studied grains (Figure 9c) or to glauconite intergrowth with 7 Å phases (Amouric et al. 1995).

The trial has been made to evaluate the approximate crystallochemical formulae of 7 Å phases. To do this, only Si, Al, Fe and Mg were taken into account and normalization to the total charge of octahedral and tetrahedral cations equal to 14 was applied. Because it is impossible to determine the oxidation state of Fe for individual flakes and by using the Mössbauer data obtained from bulk sample 191 (Giresse et al. 1987) it is risky, but the two assumptions were initially made: 1) either all Fe is Fe³⁺; or 2) all Fe is Fe²⁺.

The 7 Å phases (Table 2) were classified using the projection system of chemical composition (Wiewióra 1990a and 1990b). The points corresponding to the crystallochemical formulae, calculated on the basis Fe³⁺ lie in the proximity of the kaolinite end member (Figure 11). No doubt, such formulae 3 to 6 are unrealistic because the projection points are far from the $d(060)$ values estimated by XRD (Figure 11, crosses). With the assumption of Fe²⁺, these projection points fall closer to isoline of $d(060)$ equal to approximately 1.55 Å (formula 5) and closer to 1.535 Å (formulae 3, 4 and 6).

Using the X-ray determined $d(060)$ values (Figures 6, 7 and 9) Figure 11 offers the most probable compositions of 7 Å phases. For example, for sample number 6, analyzed by EDAX and XRD the determined value of $d(060) = 1.535 \text{ Å}$ (Figure 9b), the chemical composition is given by the crystallochemical formula $(R^{3+}_{1.23} R^{2+}_{1.22})(Si_{1.88} R^{3+}_{0.12} O_5(OH)_4$ where: $R^{3+} = Al, Fe^{3+}$; $R^{2+} = Mg, Fe^{2+}$. Point 1 [$d(060) = 1.504 \text{ Å}$] is

Table 2. Average chemical composition and structural formulae of 7 Å phases within Recent and Miocene grains. Each analysis represents the average value from 8 or more points.

Element	Recent			Miocene		
	1	2	3	4	5	6
Mg	1.08	3.03	3.87	3.67	13.43	2.97
Al	2.46	6.69	10.20	8.65	10.19	8.38
Si	18.09	17.79	21.75	20.05	17.33	18.14
Fe	10.36	23.67	21.44	26.97	15.84	25.10
Fe_{total} as Fe³⁺						
Si	1.96	1.85	1.90	1.79	1.55	1.77
Al ^{IV}	0.04	0.15	0.10	0.21	0.45	0.23
Al ^{VI}	1.36	0.57	0.83	0.60	0.50	0.62
Fe ³⁺	0.56	1.24	0.94	1.21	0.71	1.23
Mg	0.14	0.36	0.39	0.39	1.39	0.34
ΣR ³⁺	1.92	1.81	1.77	1.81	1.21	1.85
ΣR ²⁺	0.14	0.36	0.39	0.39	1.39	0.34
□	0.94	0.83	0.83	0.80	0.38	0.81
Fe_{total} as Fe²⁺						
Si	2	2	2	1.96	1.64	1.94
Al ^{IV}	—	—	—	0.04	0.36	0.06
Al ^{VI}	1.46	0.79	0.99	0.84	0.64	0.87
Fe ²⁺	0.59	1.35	1.01	1.32	0.75	1.35
Mg	0.14	0.40	0.42	0.40	1.45	0.37
ΣR ³⁺	1.46	0.79	0.99	0.84	0.64	0.87
ΣR ²⁺	0.73	1.75	1.43	1.72	2.20	1.72
□	0.73	0.40	0.50	0.40	1.14	0.40

very close to kaolinite, but more precisely to the Fe-bearing kaolinite of Amouric et al. (1995). Crystallochemical formulae 3, 4 and 6 corresponding with projection points of $d(060) = 1.535$ Å fall within the field

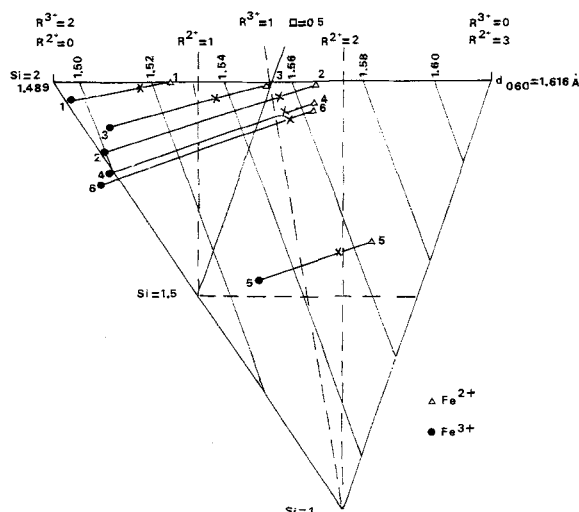


Figure 11. Projection of chemical compositions given by crystallochemical formulae (Table 3) corresponding with $d(060)$: Key: 1 and 2 = kaolinite from Recent grains; 3 and 4 = 7 Å phases in Miocene grains -370 m and -520 m depth; 5 = trioctahedral 7 Å phases (quasi-berthierine) in Miocene grain -185 cm; 6 = 7 Å phases in Miocene grain -230 m X-ray analyzed (Figure 9b); x = compositions corresponding to $d(060)$ equal 1.504 Å (1.2), 1.535 Å (3, 4, 6), 1.55 Å (5); Δ = Fe taken as Fe²⁺; and ● = Fe taken as Fe³⁺.

for dioctahedral serpentines, but are very close to the boundary with trioctahedral species (□ = 0.5). They represent the crystallochemical formulae of the partially transformed phases in which cation substitution of Mg and Fe for Al are within the octahedral sheet, but only some substitution of Al for Si within the tetrahedral sheet is observed. Transformation proceeds more toward the greenalite apex than the Mg-berthierine end-member position for the project field, except for point 5, which is in the center of the field for trioctahedral species not far from berthierine.

The application of the projection field for chemical composition and $d(060)$ value, measured by the diffraction method, appears to be the best way to estimate the crystallochemical formulae of Fe-containing minerals when determination of the oxidation state of Fe is not possible. Using this approach one may go a little further in the trial to estimate the crystallochemical formulae. Namely the knowledge of ΣR²⁺ and ΣR³⁺ enables the scientist to calculate the partition of Fe into Fe²⁺ and Fe³⁺ (Table 3). This way we show that in the Recent grains Fe³⁺ prevails over Fe²⁺. When Al content in octahedral position is very high (Table 3, column 1) the Fe content is low and Fe occurs mostly as Fe³⁺. In Miocene grains, divalent Fe prevails over trivalent. This gives rise to the supposition concordant with the findings of Amouric et al. (1995) concerning different methods of formation of Fe-bearing kaolinite and 7 Å trioctahedral phases by solid state transformation of kaolinite and by local dissolution and neof ormation.

Table 3. Average chemical composition and structural formulae of 7 Å phases within Recent and Miocene grains recalculated from Table 2.

Element	Recent		Miocene		
	1	2	3	4	5
Mg	1.08	3.03	3.87	3.67	13.43
Al	12.46	6.69	10.20	8.65	10.19
Si	18.09	17.79	21.75	20.05	17.33
Fe	10.36	23.67	21.44	26.97	15.84
Si	1.96	1.87	1.96	1.88	1.61
Al(IV)	0.04	0.13	0.04	0.12	0.39
Al(VI)	1.38	0.60	0.94	0.72	0.57
Fe ³⁺	0.50	1.11	0.40	0.60	0.34
Fe ²⁺	0.06	0.14	0.60	0.68	0.39
Mg	1.14	0.36	0.41	0.40	1.44
Σ _{octa} 3+	1.88	1.77	1.34	1.32	0.91
Σ _{octa} 2+	0.20	0.50	1.01	1.08	1.78
□	0.92	0.79	0.65	0.60	0.26

SMECTITES. Within the Recent and Tertiary grains, the neof ormation of smectites was observed under the electron scanning microscope (Figure 8). The recorded chemical elemental spectra showed very little variation for composition: high Si, Al, Fe, low Mg, K and Ca content. For more detailed evaluation of their chemical composition by EDAX technique, smectites forming cabbage-like structures within Miocene grains were chosen. Chemical analyses were made on 3 smectite flakes for each of the 3 grains, with 2 coming from -180 m and 1 from -220 m samples. The crystallochemical formulae, assuming total Fe as ferric, were calculated normalizing the total cation charges to 22. The resulting crystallochemical formulae are presented in Table 1.

Octahedral Fe, expressed in number of atoms per half unit cell, and the b unit cell parameters determined from the measured $d(060) = 1.524$ Å were used for a Brigatti plot (Stucki 1988). In Figure 10, it is shown that the projected point for our smectites conforms well with the relationship between octahedral Fe and the b dimension of the unit cell of Fe-rich nontronite. This, apart from morphology, proves again that the K containing neof ormed smectite within green grains is the nontronite.

DISCUSSION AND CONCLUSIONS

Environmental Factors

RECENT DEPOSITS. This example of the shelf beyond the mouth of the Congo-Zaire River shows that grains with 7 Å layers are not always located within deltaic deposits below -60 m (Odin and Sen Gupta 1988). Here the peloids with 7 Å layers are observed on the outer shelf where the sedimentation rate is higher. Thus, factors of hydro-sedimentation are believed to be more important than bathymetry *sensu stricto*. The northern outer shelf with a lower sedimentation rate, is propitious for nontronite neof ormation.

HOLOCENE SEQUENCE. The 4 studied horizons from the core show with decreasing depth, the disappearance of kaolinites on behalf of 7 Å Fe-bearing phases. Such disappearance is related to the sedimentation rate: in the upper part formed during the slower deposition rate, seawater-sediment interaction was developed and it favored an early diagenetic process.

MIOCENE DEPOSITS. Five hundred to 700 m below the subsurface, within shallow marine deposits, pellets have been found that differ slightly from the Recent and Holocene ones, nontronite is nearly equal in content to 7 Å phases, whereas quartz is relatively rare. The composition suggests that some further processes have occurred with burial. The formation of phases with better ordered structures takes place at higher temperatures and pressures, than those prevailing at the depth at which these Miocene peloids were found.

Of the 2 possible ways of further evolution of the green grains, that of glauconitization marked by neof ormation of nontronite, is more likely than that common for berthierine Fe ores marked by the formation of Mg-berthierine or greenalite like layers.

Significance of 7 Å Trioctahedral Phases

X-ray measurement of $d(060)$ spacing, by transmission diffractometry and EDAX chemical composition studies of morphologically different mineral flakes, proved the persistence of several 7 Å phases, different from kaolinite with respect to chemical composition and b dimension of the unit cell. The differences in the b dimension are displayed in a series of $d(060)$ values: 1.488 Å common for kaolinite, 1.504 Å common for Fe-bearing kaolinite, 1.537 Å and 1.55 Å common for 7 Å di-trioctahedral and trioctahedral phases. This increase of $d(060)$ value resulted from the substitution of Al by Fe and Mg in octahedra, accompanied by some Al migration from octahedral to tetrahedral sheets in 1:1 layers, as followed from chemical compositions of serpentine-kaolinite phyllosilicates represented in Figure 11.

The 7 Å phases with different b dimensions are present not only in Miocene peloids, but also in the Recent superficial ones from deposits with low sedimentation rates.

Degradation of kaolinite structure accompanied by partial introduction of Fe³⁺ in octahedral positions was observed during tropical weathering in lateritic profiles (Nahon 1981; Jepson 1988). Degraded kaolinite with Fe³⁺ within octahedra was encountered during the initial stages of transformation, observed within Recent grains with a rather negligible content of Fe²⁺. For more developed phases of transformation, observed here within Miocene grains, Fe²⁺ prevailed over Fe³⁺ and the Mg content was also high (Table 3). The differences are due to totally different environmental conditions, in the tropical zone, on the conti-

ment and in the ocean. The latter is characterized first of all by: 1) organic matter present in mud and in the micro environment of fecal pellets, which controls fronts of oxidation/reduction potential; 2) Mg concentration in marine waters causing instability and creating conditions for the migration of Al from octahedra of 7 Å phases (Table 2).

The 7 Å phases, which are the major phyllosilicate constituents of the grey-green grains from the Congo continental margin may be compared to odinite from the Island of Loss, off Guinea. However, it should be noticed that odinite generally occurs as a green pigment on coarse grained bioclastic sand and infillings for bioclastics from the New Caledonia and Senegal southern continental shelf (Odin 1988), where sedimentation conditions are different from those on the Congo shelf. They are characterized by insignificant ferruginous influx and circulating currents, and by the deposition of fine, particulate matter derived from the weathering products of mafic rocks that seem to be the primary material for the formation of the New Caledonian odinite. A very active ferruginous sedimentary environment is believed to be the most significant for the formation of Congolese green grains; mud, rich in Fe and carbon (Giresse 1985) is the primary material.

Nontronite forming cabbage-type structures, composed from very fine flakes (Figure 8), evidently neoformed, has a very stable b dimension of the unit cell, contrary to 7 Å phases. It crystallizes from Si gels (Parron 1989) rich in Fe and Al, derived from the degradation of micas and other accessory minerals unstable in marine conditions. It contains K as the principal exchangeable cation, which is typical for smectites crystallized in a marine environment (Drits 1992).

ACKNOWLEDGMENTS

The authors express their gratitude to B. Velde for critical reading and fruitful discussion of the first version of this manuscript and to D. Grabska for technical help and to R. Hutchinson for the language corrections.

REFERENCES

- Amouric M, Parron C, Casalini L, Giresse P. 1995. A (1:1) 7 Å phase and its transformation in Recent sediments: an HRTEM and AEM study. *Clays Clay Miner* 43:446–454.
- Bailey SW. 1988. Odinite, a new dioctahedral-trioctahedral Fe³⁺ rich 1:1 clay mineral. *Clay Miner* 23:237–247.
- Bhattacharyya D. P. 1983. Origin of berthierine in ironstones. *Clays Clay Miner* 31:173–182.
- Brigatti MF. 1985. Relationships between composition and structure in Fe-rich smectites. *Clay Miner* 18:177–186.
- Brindley GW. 1980. Order-disorder in clay mineral structures. Ch. 2. In: Brindley GW, Brown G, editors. *Crystal structures of clay minerals and their X-ray identification*. London: Mineralogical Society. P 125–195.
- Brindley GW. 1982. Chemical composition of berthierine—a review. *Clays Clay Miner* 30:152–155.
- Cotter E. 1992. Diagenetic alteration of chamosite minerals to ferric oxide in oolitic limestone. *J Sedim Petrol* 62:54–60.
- Drits VA. 1992. Interviews with the clay scientists. CMS News, February 1992. p 9.
- Giresse P. 1985. Le fer et les glauconies au large du fleuve Congo. *Strasbourg: Sci Géol* 38:293–322.
- Giresse P, Wiewióra A, Lacka B. 1987. Migration des éléments et minéralogénèse dans les grains verts Récents au large de l'embouchure du Congo. *Archiw Mineral* 42:5–30.
- Giresse P, Wiewióra A, Lacka B. 1988. Mineral phases and processes within green peloids from two recent deposits near the Congo River mouth. *Clay Miner* 23:447–458.
- Giresse P, Oualembo P, Wiewióra A, Lacka B, Zawadzki P. 1992. Compositions polyphases des grains verts du Bassin du Congo; Comparaison des depots Recents, Holocenes (103–104 ans) et Miocenes (107 ans). *Archiw Mineral* 47:17–50.
- Ijima A, Matsumoto R. 1982. Berthierine and chamosite in coal measures of Japan. *Clays Clay Miner* 30:264–274.
- Jepson WB. 1988. Structural iron in kaolinities and in associated ancillary minerals. In: Stucki JW, Goodman BA, Schwertmann U, editors. *Iron in soils and clay minerals*. Dordrecht: Reidel D. P 467–536.
- Nahon D. 1981. Modes de répartition des métaux dans les solutions solides des altérations tropicales; application aux concentrations supergènes ferrugineuses. In: Nahon D, editor. *Valorisation des ressources du sous-sol*, Orléans: Doc BRGM 47. 254–264.
- Odin GS. 1985. La "verdine", faciès granulaire vert, marin et côtier, distinct de la glauconie: distribution actuelle et composition. *Paris: CR Acad Sc* 301, 2:105–108.
- Odin GS. 1988. The verdine facies from the lagoon off New-Caledonia. In: Odin GS, editor. *Green marine clays. Developments in Sedimentology*. Amsterdam: Elsevier. p 57–81.
- Odin GS, Sen Gupta BK. 1988. Geological significance of the verdine facies. In: Odin GS, editor. *Green marine clays. Developments in Sedimentology* 45. Amsterdam: Elsevier. P 205–219.
- Parron C. 1989. Voies et mécanismes de cristallogénèse des minéraux argileux ferrifères en milieu marin. Le processus de glauconitisation: évolutions minérales, structurales et géochimiques. [PhD Thesis]. Aix-Marseille: Sc Univ. III. 411 p.
- Stucki JW. 1988. Structural iron in smectites. In: Stucki JW, Goodman BA, Schwertmann U, editors. *Iron in soils and clay minerals*. Dordrecht: Reidel D. p 625–675.
- Velde B. 1989. Phyllosilicate formation in berthierine peloids and Iron oolites. In: Young TP, Taylor WEG, editors. *Phanerozoic Ironstones*. London: Geological Society 46. p 3–8.
- Vila E, Ruiz-Amil A, Martin de Vidales JL. 1988. Computer programs for X-ray powder diffraction analysis. Madrid: Internal Report CSIC. 17 p.
- Wiewióra A. 1990a. Crystallochemical classifications of phyllosilicates based on the unified system of projection of chemical composition. I. The mica group. *Clay Miner* 25:73–81.
- Wiewióra A. 1990b. Crystallochemical classifications of phyllosilicates based on the unified system of projection of chemical composition. III. Serpentine-kaolin group. *Clay Miner* 25:93–98.

(Received 8 November 1995; accepted 3 December 1995; Ms. 2593)